Wiley Online Library
Early View publication on www.wileyonlinelibrary.com
(issue and page numbers not yet assigned;
citable using Digital Object Identifier – DOI)

J. Biophotonics 1–7 (2016) / **DOI** 10.1002/jbio.201500263

Journal of BIOPHOTONICS

FULL ARTICLE

Quantitative phase measurements of tendon collagen fibres

Dylan Maciel[1], *Samuel P. Veres*[2, 3], *Hans Juergen Kreuzer*[1], *and Laurent Kreplak*[*, 1, 3]

[1] Department of Physics and Atmospheric Science, Dalhousie University, Halifax, NS, B3H 4R2, Canada
[2] Division of Engineering, Saint Mary's University, Halifax, NS, B3H 3C3, Canada
[3] School of Biomedical Engineering, Dalhousie University, Halifax, NS, B3H 4R2, Canada

Received 2 October 2015, revised 18 December 2015, accepted 22 December 2015
Published online 30 January 2016

Key words: Optical index, collagen, water content, diameter, heat treatment, tensile overload

Collagen is the main component of structural mammalian tissues. In tendons, collagen is arranged into fibrils with diameters ranging from 30 nm to 500 nm. These fibrils are further assembled into fibres several micrometers in diameter. Upon excessive thermal or mechanical stress, damage may occur in tendons at all levels of the structural hierarchy. At the fibril level, reported damage includes swelling and the appearance of discrete sites of plastic deformation that are best observed at the nanometer-scale using, for example, scanning electron microscopy. In this paper, digital in-line holographic microscopy is used for quantitative phase imaging to measure both the refractive index and diameter of collagen fibres in a water suspension in the native state, after thermal treatments, and after mechanical overload. Fibres extracted from tendons and subsequently exposed to 70 °C for 5, 15, or 30 minutes show a significant decrease in refractive index and an increase in diameter. A significant increase in refractive index is also observed for fibres extracted from tendons that were subjected to five tensile overload cycles.

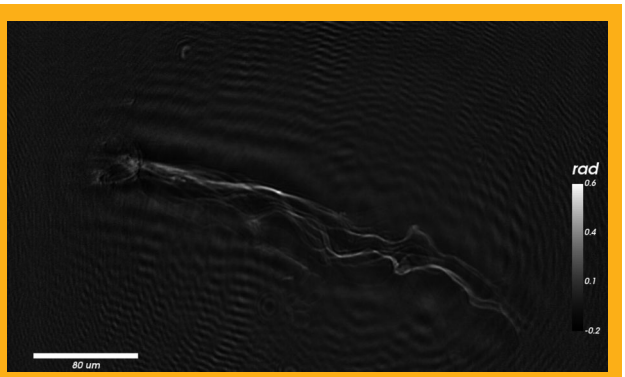

1. Introduction

Collagen is the most abundant protein in the animal kingdom, providing structural integrity to tissues in the form of fibrillar scaffolding. Collagen molecules form fibrils with diameters between 30 nm and 500 nm depending on tissue type and developmental stage. In humans, the two extremes in this spectrum are the cornea, which is transparent with a narrow distribution of 30 nm wide fibrils [1], and tendons, which are opaque and have a broad, often-bimodal distribution that covers the entire width range [2]. In tendons, fibrils are arranged in helical fibres with diameters of several micrometers [3] that are in turn packed into fascicles [2].

* Corresponding author: e-mail: kreplak@dal.ca

Due to the abundance of collagen fibril-based tissues within the human body, many diseases and ailments involve structural changes to collagen at various levels of structural hierarchy. Examples include tendinopathy, ligament rupture, osteoarthritis, intervertebral disc degeneration, diabetes, aneurysm, tumor development, etc. While microstructural changes to collagenous tissues can be readily assessed using tools like optical microscopy, ultrasound, and magnetic resonance imaging, there are currently a limited number of ways to quantitatively study nano-structural changes. New methods of assessing the nanostructures of these tissues could enable a more complete understanding of numerous pathologies, and offer new possibilities for diagnostic assessment.

Measuring a tissue's refractive index may provide a new means for assessing structural damage. Using optical coherence tomography (OCT), the refractive index of brain tissue has been shown to increase significantly with increasing compressive force applied to the tissue [4]. In bovine articular cartilage, refractive index measurements using OCT have been shown to vary with structural changes caused by trypsin digestion [5]. The main drawback of OCT in determining the refractive index is the need to have an independent measurement of the sample thickness [4]. One way to overcome this issue is to implement quantitative phase imaging (see [6] for a review). One version of this approach is digital in-line holographic microscopy (DIHM), which allows the direct measurement of phase-shifts between a microscopic sample and its surrounding medium [7]. For objects with simple geometries such as plates, spheres, and cylinders, DIHM can be used to measure both the object's refractive index and physical dimensions, as recently demonstrated for the first time using E. coli and the core of a fibre optic cable [7]. This technique has now also been used to study the time dependence of HEK 293 cell death induced by exposure to hydrogen peroxide [8].

In this study we have used DIHM to measure the refractive index and diameter of collagen fibres extracted from bovine tail tendons. In order to assess the ability of DIHM to quantitatively identify structural changes to collagen tissues, measurements of collagen fibres subjected to heat treatment and mechanical overload, both of which are known to cause nano-structural changes [9–12], have also been taken. Our results show that thermal treatment of the fibres or tensile overload of the tendon before fibre extraction significantly decreases the refractive index with respect to untreated fibres. These results support the potential use of DIHM for assessment of structural change in collagenous tissues.

2. Materials and methods

2.1 Collagen samples

Two tendons were dissected from the dorsal, proximal region of the tail of a 24–36 month-old steer that was slaughtered for food (Oulton Farms, Nova Scotia, Canada). The dissected tendons were laid flat between sheets of gauze moistened with phosphate buffer saline (PBS) and stored at −86 °C until further use. Each tendon was thawed by immersion in a large volume of PBS at room temperature and cut into two pieces.

The first piece was rinsed in de-ionized water and dissected further using tweezers and a fine tipped glass rod in several millilitres of water until small clumps of collagen fibres were visible. The dilute collagen suspension was separated into four 1 ml samples. One was kept at room temperature while the three others were heated in a water bath at 70 °C, for 5, 15, and 30 minutes, respectively. Once cooled, a small volume of each sample including some visible clumps was mounted between a regular microscope slide and a thin cover glass.

The second piece of each tendon was overloaded in tension. Before overloading, each piece of tendon was first vertically suspended and photographed four times at axial rotation increments of 90°. The four photos were then used to calculate each tendon's elliptical cross-sectional area. Each tendon was then mounted in the grips of a servo-hydraulic materials testing system using an intergrip gauge length of 15 mm. At a strain rate of 0.5%/s, each tendon was subjected to five cycles of repeated tensile overload, as described previously [11, 13]. Briefly, using custom written software programmed under LabVIEW, each tendon was stretched until the slope of its load-deformation response reached zero. The actuator then reversed, unloading the tendons at the same rate of 0.5%/s. Upon reaching the zero displacement position, the next loading cycle began immediately. During testing, tendons were kept hydrated via a regular application of PBS droplets. After the five subrupture overload cycles were complete, each tendon was then rinsed in de-ionized water and dissected as described above to free collagen fibres.

2.2 Digital in-line holography

Holograms of each sample were taken using a point source digital in-line holographic microscope (4deep, Halifax, Canada). A schematic is shown in Figure 1: The light source is either a pinhole or the core of a fibre optic cable, as in the instrument used for this work. The pinhole or cable has a diameter on the

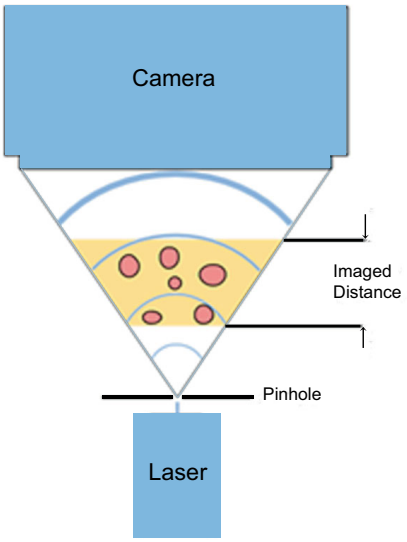

Figure 1 Schematic of the DIHM set-up used in this study. In our case, the laser has a wavelength of 400 nm and a single mode optical fibre of 1.6 μm diameter replaces the pinhole.

order of the illuminating laser's wavelength. The emerging light is a cone of a spherical wave with a numerical aperture NA = $0.62\lambda/r$, with λ the wavelength of light and r the radius of the source. This primary light wave scatters off the objects in its path creating an object wave, which interferes with the primary wave to form a hologram on a CCD camera, provided the scattered wave is small compared to the primary wave. The hologram is then reconstructed on many planes throughout the object space using the Kirchhoff–Helmholtz transform, from which both intensity and phase maps are obtained.

In our case, the light source of the microscope consisted of a 400 nm wavelength pulsed laser connected to a single mode optical fibre with a 1.6 μm diameter core (numerical aperture of this "point" source is NA = 0.3). The spherical wave emanating from the tip is scattered by the sample, which was typically positioned 1 mm away from the point source. The reference wave and scattered wave from the sample interfere to form a hologram that was collected with a μToshiba Teli CSB 4000F-20 CCD camera. For each sample, we acquired multiple holograms in the periphery of visible clumps of collagen fibres. Intensity and phase images at different planes throughout the sample volume were reconstructed using Octopus software (v1.6.0, 4deep, Halifax, Canada) to find the plane where the fibre was in focus.

For quantitative analysis of the collagen fibres we used reconstructed phase images of single fibres in their focal plane and took several radial cross sections through the fibre. Because collagen fibres are not homogeneous we took anywhere from one to five phase cross sections per fibre. In total we collected 50 phase cross-sections per sample type, per tendon.

We modelled the fibres as cylinders of radius R with a refractive index difference with respect to water of Δn. If we call r the lateral distance from the centre of the fibre, the change in phase experienced by the reference wave, of wavelength λ, going through the fibre is $\Delta\varphi$:

$$\Delta\varphi = \frac{4\pi\,\Delta n}{\lambda}\sqrt{(R^2 - r^2)} \qquad (1)$$

For further analysis the phase profiles were squared to prevent complex roots and then fitted with the square of Eq. (1). The model predicts a very sharp increase in phase on the sides of the cylinder that was not observed experimentally due, in part, to the Gaussian-type point-spread function that accounts for the finite numerical aperture of the instrument. This broadening can be removed numerically be a deconvolution as shown elsewhere [14]. For the present work this step can be avoided (because of the simple rod-like geometry of the objects) by fitting the data points within the full-width at half maximum from the centre of the fibre.

2.3 Statistics

Statistical analyses were conducted using JMP software (version 11.0.0, SAS Institute Inc.). First, in cases where multiple measurements had been performed on the same fibre, the resulting values were averaged, producing a single value of diameter and refractive index contrast for each fibre. For both responses (fibre diameter and refractive index contrast), Shapiro-Wilk tests confirmed that the data for several treatment groups were not normally distributed, and Leven's test confirmed unequal variances between the treatment groups. Therefore, the effect of treatment on each response was analyzed for significance using a non-parametric Kruskal-Wallis test, followed by Wilcoxon rank-sum tests. To account for the multiple Wilcoxon rank-sum tests needed to compare the five treatments for each response, the p-value required for statistical significance was adjusted using a Bonferroni correction to $p \leq 0.005$. Correlations between fibre diameter and refractive index contrast were fit using linear regressions, and tested for significance using t-tests.

3. Results

In total, diameter and refractive index contrast measurements were made on 34 control collagen fibres,

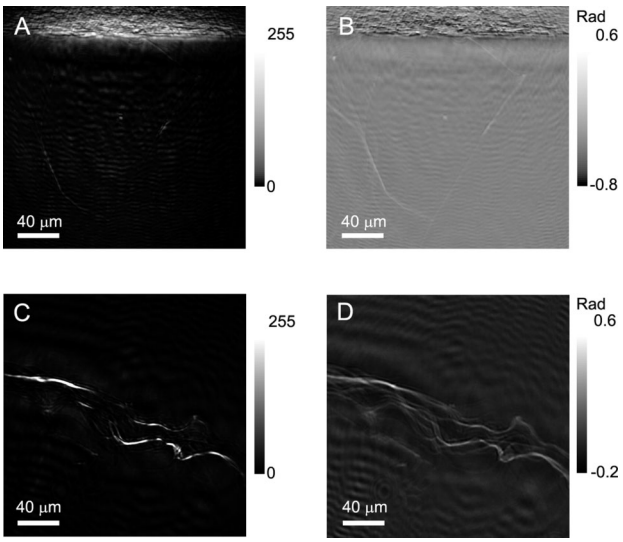

Figure 2 Intensity and phase reconstructions of the same area of a control sample (**A**, **B**) and of an overloaded sample (**C**, **D**). The holograms are acquired with a source-screen distance of 22 mm. The in focus reconstruction plane is 725 µm above the source in both cases. The bright structure at the top of the intensity reconstruction in (**A**) is a large bundle of collagen fibres. Individual collagen fibres are barely discernible in the intensity reconstruction and clearly visible in the phase reconstruction.

41 fibres that had been heated at 70 °C for 5 min, 41 fibres that had been heated at 70 °C for 15 min, 45 fibres that had been heated at 70 °C for 30 min, and 32 fibres from two tendons that had undergone repeated subrupture overload.

Holograms obtained with DIHM allow the reconstruction at any plane within the sample volume of both intensity and phase. It should be noted that due to the transparency of single collagen fibres in water they are seldom visible in the reconstructed intensity images, but are easily identified in the phase reconstructions (Figure 2A vs. B, and 2C vs. D). Because of the weak scattering and micron size of the fibres, we operate at the resolution limit of optical microscopy. Consequently, ripple-like artifacts are produced, but are easily identified as such (Figure 2B, D). They could be avoided by using a larger numerical aperture, i.e. a shorter wavelength or a thinner optical fibre. In the present study they were tolerable: to ensure that the artifacts did not interfere with our measurements, profiles were only taken at locations where the phase remained approximately zero a few micrometers away from the centre of the fibre. (Figure 3A). For these profiles, a least-square fit of Eq. (1) to the upper half of the profile provides the fibre radius R and the refractive index contrast Δn (Figure 3B and C).

For the control samples, the diameter of the collagen fibres that were reconstructed varied between 1.4 µm and 2.2 µm (Figure 4A) while their refractive index contrast with respect to water varied between 0.007 and 0.023 with an average of 0.014 ± 0.005 (Figure 4B). Fibres smaller than 1.4 µm are visible in some phase reconstructions but the profiles are too noisy to be reliably fitted. Fibres larger than 2.2 µm are typically visible in intensity reconstructions but their corresponding phase reconstructions are saturated. In other words, the observed diameter range is limited by the experimental constraints and does not fully represent the size distribution in the sample. Within the 1.4 µm to 2.2 µm fibre diameter range analyzed in this experiment, there was no correlation between fibre diameter and refractive index contrast (Figure 5).

Exposure to 70 °C caused a significant increase in fibre diameter. Heating for 5, 15, and 30 minutes increased the mean fibre diameter by 24%, 29%, and 35%, respectively (Figure 4A). Thermal treatment had an even larger effect on refractive index

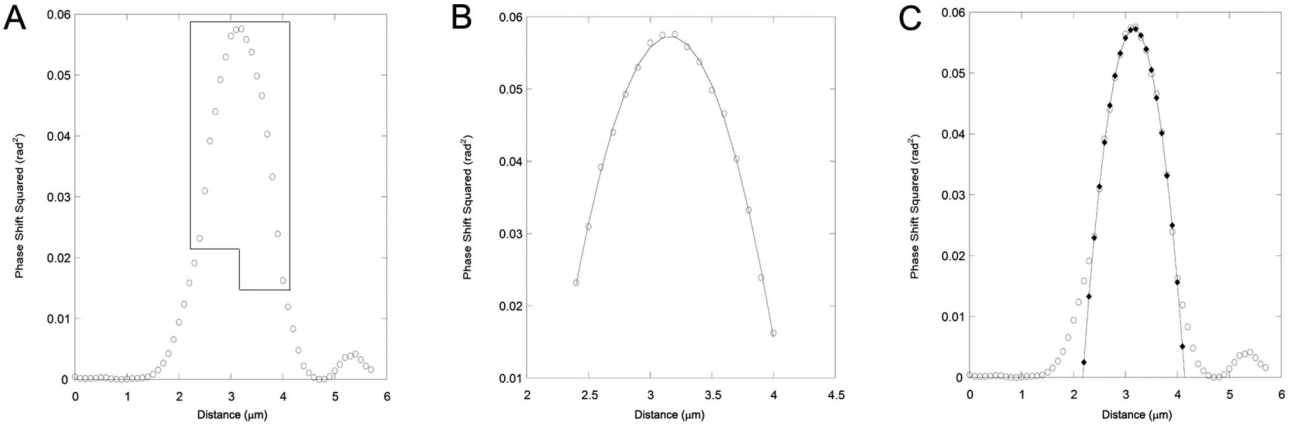

Figure 3 (**A**) Square of a phase profile obtained by taking a radial cross section from a phase reconstruction of one hologram. (**B**) Data points within the region indicated in (**A**) are fit using Eq. (1). (**C**) The fit plotted together with the entire squared phase profile. The flaring at the edges of the fibre is due to the point spread function of our instrument.

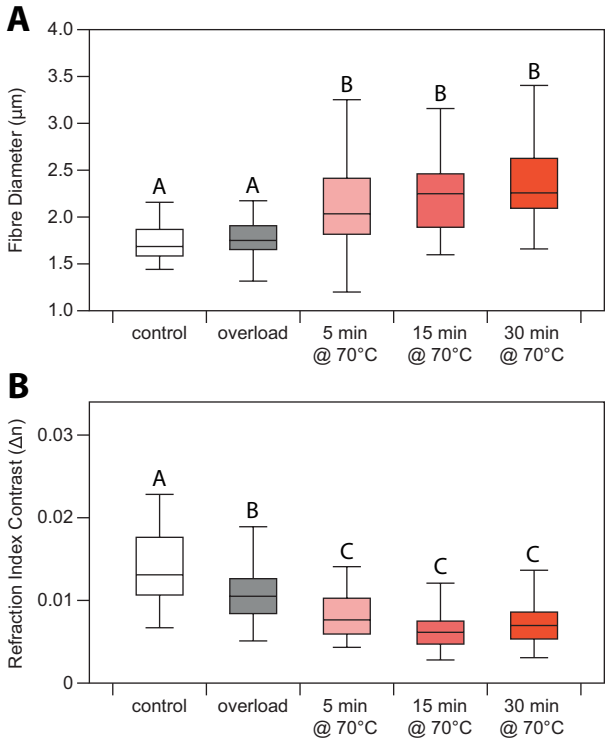

Figure 4 Summary of the fibre diameter (**A**) and refractive index contrast relative to water (**B**) for profiles taken on tendon collagen fibres from 5 sample groups: control, tensile overload followed by fibre extraction, fibre extraction (as for the control) followed by heat treatment at 70 °C for 5, 15, or 30 min. (**A**) Diameter of the fibres as a function of the different treatments. (**B**) Refractive index contrast as a function of the different treatments. Different letters indicate significant differences between treatment groups ($p \leq 0.005$). The refractive index of water at a wavelength of 400 nm is 1.339 [15].

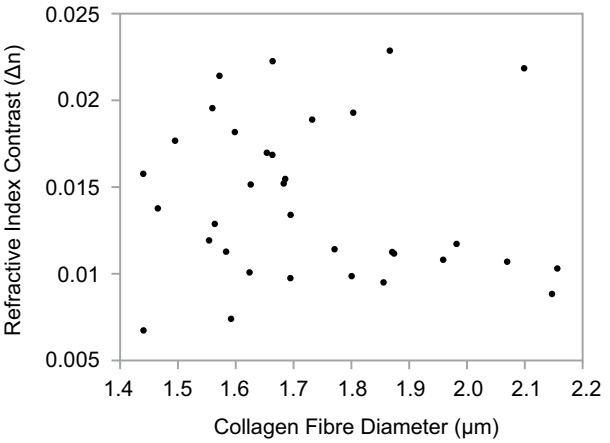

Figure 5 Refractive index contrast versus diameter of the collagen fibres measured from the control sample. There is no obvious correlation between the two quantities.

contrast. Heating for 5, 15, and 30 minutes caused mean decreases of 43%, 57%, and 50%, respectively, all of which were significant relative to the control samples, but not statistically different from one another (Figure 4B).

For the first cycle of subrupture tensile overload, one tendon reached a maximum stress of 30.3 MPa at a strain of 24.7%. The other tendon reached a maximum stress of 51.0 MPa at a strain of 18.9%. As expected from previous experiments [11, 13], progressively smaller maximum stresses, and larger maximum strains were recorded during the subsequent four overload cycles. Tensile overload did not affect fibre diameter, but significantly reduced refractive index contrast, causing a mean decrease of 21% relative to the control samples (Figure 4).

4. Discussion

The refractive index of water at a wavelength of 400 nm is 1.339 [15]. Based on our measured phase-shifts we can assign an average refractive index to fully hydrated bovine tail tendon collagen fibres of 1.353 ± 0.005. The observed range of refractive index from 1.346 to 1.362 matches that of fully hydrated bovine posterior corneal stroma, which was previously found to range from 1.345 to 1.365 [16]. Considering that the two systems have completely different collagen fibril architecture [1–3], one can safely assume that the refractive index of a densely packed array of native collagen fibrils in water is between 1.35 and 1.37.

If the structure of the collagen fibrils were disturbed in such a way that they absorb more water, one would expect the refractive index to decrease. In our experiments, disrupting collagen fibres via heat treatment lowered the refractive index, from an average of 1.353 ± 0.005 for the control samples to 1.345 ± 0.002 for samples heated at 70 °C for 15 minutes. Here, the absolute change in refractive index due to heat treatment is around 0.6% corresponding to a variation in refractive index of 0.008 that is clearly resolved by DIHM. This variation is eight times larger than the highest accuracy achieved so far with the DIHM technique, which is 0.001 [7] i.e. well within the range of its resolution. Neglecting the contribution of dissolved individual collagen molecules to the refractive index of the surrounding water, the observed decrease in refractive index contrast with heating may be attributed to an uptake of water by the thermally treated fibres. This explanation is consistent with the observation of single fibril swelling after exposure to a temperature of 62 °C, cooling, and subsequent AFM imaging in water [12]. In this particular study, two fibrils were imaged and the increase in diameter was 20% and 30%, respec-

tively [12]. A similar swelling of collagen fibrils has also been observed in pig corneal stroma exposed to temperatures above 60 °C [17]. For the fibres extracted from overloaded tendons, the observed decrease in refractive index contrast can be similarly explained. Previous work has shown that the repeated overload regime used here causes collagen fibrils to enlarge as their periphery undergoes molecular denaturation [11].

In addition to changes in water content, collagen denaturation – uncoiling of the collagen molecule's native triple-helix – may have also contributed to the changes in refractive index contrast observed in the present study with heat treatment and mechanical overload. The thermal denaturation of adult bovine tail tendons, the same tissue model used in this study, has previously been studied [13, 18]. As assessed by hydrothermal isometric tension testing, collagen molecules within adult bovine tail tendons begin denaturing at 63.5 °C [13]. A similar onset temperature for molecular denaturation has been found using differential scanning calorimetry [18]. In addition to the start of denaturation, the endotherm produced during differential scanning calorimetry also allows the completion of denaturation to be measured. For bovine tail tendons, denaturation is largely complete by 70 °C when a scanning rate of 5 °C/minute is used [18]. At a constant temperature of 70 °C then, bovine tail tendon samples fully denature in <1.5 minutes. In the present study, collagen fibres from bovine tail tendons were exposed to 70 °C for 5, 15, and 30 minutes. It is very likely that the fibres in all of these treatment groups contained a high fraction of denatured collagen molecules. Consistent with this estimation, no difference in refractive index contrast was observed between any of the thermal treatment groups, indicating no alternation in collagen fibre structure with heating beyond 5 minutes.

If molecular denaturation does contribute to changes in the refractive index contrast of tendon, mechanical overload would be expected to have a smaller effect than thermal treatment, as was observed (Figure 4B). While the thermal treatment employed likely caused complete molecular denaturation of the tendon fibres, molecular denaturation in response to mechanical overload is known to be highly inhomogeneous. Mechanically overloading tendons only damages a subset of collagen fibrils, and within those fibrils molecular denaturation only occurs at specific locations: first within the discrete, longitudinally-repeating kinks that form, and then along the surface of the kinked fibrils [9, 13]. As a consequence, the mechanically overloaded fibres would be expected to contain a mixture of denatured and native molecules. It is not surprising, then, that the refractive index contrast for mechanically overloaded tendon fibres was found to lie between that for native fibres and thermally treated fibres.

While we did observe significant changes in refractive index contrast with both thermal and mechanical treatment in the present work, it should be emphasized that the collagen fibres used in this study were obtained from only two individual bovine tail tendons. While our results show that treatment did have a significant effect on the fibres from these particular tendons, experiments on multiple tendons from multiple individuals would be required to conclude that heat or mechanical treatments could cause measureable change in the refractive index of tendons in general.

In addition to refractive index, we have also reported the diameter of the fibres that we measured (Figure 4A). The objective in doing this is not to show how thermal or mechanical treatments affect collagen fibre diameter in tendon. Indeed, the data presented do not represent a true distribution of fibre diameter in tendon since we targeted fibres of a specific diameter range for measurement based on the imaging capabilities of our holographic apparatus. Rather, the measurements of fibre diameter illustrate that the observed change in refractive index with thermal and mechanical treatment was not due to a change in fibre diameter (Figure 5). In other words, refractive index is independent of collagen fibre diameter. Nevertheless, the observed changes in fibre diameter with treatment may be of interest. The increased diameter of the thermally treated fibres is expected as collagen molecules begin to denature, causing collagen fibrils to swell [12]. For the collagen fibres from mechanically overloaded tendon, no change in fibre diameter was observed (Figure 4). When tendons are mechanically loaded, longitudinal extension causes lateral contraction, forcing water out of the tendon [19, 20]. Upon unloading, proteoglycans within the tendon draw water back into the structure [21], restoring lateral dimensions over a period of hours [19]. In the present study, holographic measurements were made on tendon fibres three or four days after mechanical loading, providing ample time for recovery.

5. Conclusion

We have shown that the refractive index of collagen fibres of a few micrometers in diameter can be accurately measured in water with DIHM. Based on our data and the highest accuracy reported [7], DIHM can in principle detect absolute changes in refractive index of collagen fibres as small as 0.1%. This is very encouraging and could lead to a new way of monitoring minute changes in collagen matrices due to wound healing and cancer, for example, in a way that is complementary to alternative forms of struc-

tural assessment, such as second harmonic generation (SHG) microscopy.

Acknowledgements This work was made possible by an NSERC CREATE ASPIRE summer internship award to DM. SV, HJK, and LK also acknowledge support from the NSERC discovery grant program. HJK acknowledges support from the office of Naval Research (Washington, DC).

References

[1] K. M. Meek and C. Knupp, Prog. Retin. Eye Res. **49**, 1–16 (2015).
[2] J. Kastelic, A. Galeski, and E. Baer, Connect. Tissue Res. **6**, 11–23 (1978).
[3] N. S. Kalson, Y. Lu, S. H. Taylor, T. Starborg, D. F. Holmes, and K. E. Kadler, Elife **4**, 05958 (2015).
[4] J. Sun, S. Lee, L. Wu, M. Sarntinoranont, and H. Xie, Opt. Express **20**, 1084–1095 (2012).
[5] S. Wang, Y. Huang, Q. Wang, Y. Zheng, and Y. He, Connect. Tissue Res. **51**, 36–47 (2010).
[6] M. Mir, B. Bhaduri, R. Wang, R. Zhu, and G. Popescu, in: E. Wolf (ed.), Progress in Optics, Vol. 57 (Elsevier, Amsterdam, 2012), chap. 3.
[7] M. H. Jericho, H. J. Kreuzer, M. Kanka, and R. Riesenberg, Appl. Opt. **51**, 1503–1515 (2012).
[8] S. Missan and O. Hrytsenko, Proc. SPIE **9336**, 93361X/1–93361X/14 (2015).
[9] S. P. Veres and J. M. Lee, Biophys. J. **102**, 2876–2884 (2012).
[10] R. B. Svensson, H. Mulder, V. Kovanen, and S. P. Magnusson, Biophys. J. **104**, 2476–2484 (2013).
[11] S. P. Veres, J. M. Harrison, and J. M. Lee, J. Orthop. Res. **31**, 731–737 (2012).
[12] S. J. Baldwin, A. S. Quigley, C. Clegg, and L. Kreplak, Biophys. J. **107**, 1794–1801 (2014).
[13] S. P. Veres, J. M. Harrison, and J. M. Lee, J. Orthop. Res. **31**, 1907–1913 (2013).
[14] B. S. Nickerson and H. J. Kreuzer, Adv. Opt. Techn. **2**, 337–344 (2013).
[15] G. M. Hale and M. R. Querry, Appl. Opt. **12**, 555–563 (1973).
[16] K. M. Meek, S. Dennis, and S. Khan, Biophys. J. **85**, 2205–2212 (2003).
[17] P. Matteini, R. Cicchi, F. Ratto, D. Kapsokalyvas, F. Rossi, M. de Angelis, F. S. Pavone, and R. Pini, Biophys. J. **103**, 1179–1187 (2012).
[18] S. P. Veres, J. M. Harrison, and J. M. Lee, Matrix Biology **33**, 54–59 (2014).
[19] S. C. Wearing, J. E. Smeathers, S. L. Hooper, S. Locke, C. Purdam, and J. L. Cook, Br. J. of Sports Med. **48**, 383–387 (2014).
[20] K. G. Helmer, G. Nair, M. Cannella, and P. Grigg, J. Biomech. Eng. **128**, 733–741 (2006).
[21] K. Legerlotz, G. P. Riley, and H. R. C. Screen, Acta Biomaterialia **9**, 6860–6866 (2013).